

## A Novel Synthesized Tyrosinase Inhibitor: (*E*)-2-((2,4-Dihydroxyphenyl)diazenyl)phenyl 4-Methylbenzenesulfonate as an Azo-Resveratrol Analog

Sung Jin BAE,<sup>1,\*</sup> Young Mi HA,<sup>1,\*</sup> Jin-Ah KIM,<sup>2</sup> Ji Young PARK,<sup>2</sup> Tae Kwun HA,<sup>3</sup> Daeui PARK,<sup>1</sup> Pusoon CHUN,<sup>4</sup> Nam Hee PARK,<sup>5</sup> Hyung Ryong MOON,<sup>2</sup> and Hae Young CHUNG<sup>1,†</sup>

<sup>1</sup>Molecular Inflammation Research Center for Aging Intervention (MRCA), College of Pharmacy, Pusan National University, Kumjeong-gu, Busan 609-735, Republic of Korea

<sup>2</sup>Laboratory of Medicinal Chemistry, College of Pharmacy, Pusan National University, Busan 609-735, Republic of Korea

<sup>3</sup>Department of Surgery, Busan Paik Hospital, College of Medicine, Inje University, Busan 614-735, Republic of Korea

<sup>4</sup>College of Pharmacy, Inje University, Gimhae, Gyeongnam 621-749, Republic of Korea

<sup>5</sup>Department of Nursing, College of Medicine, Inje University, Busanjin-gu, Busan 633-165, Republic of Korea

Received July 19, 2012; Accepted September 26, 2012; Online Publication, January 7, 2013

[doi:10.1271/bbb.120547]

We synthesized a novel series of (*E*)-2-((substituted phenyl)diazenyl)phenyl 4-methylbenzenesulfonate derivatives (2 and 3) and (*E*)-2-((substituted phenyl)diazenyl)phenol derivatives (4 and 5), and conducted an evaluation in order to determine their inhibitory effects on mushroom tyrosinase, with the aim of discovering a tyrosinase inhibitor. Most of the compounds (3–5) exhibited higher inhibitory effects than kojic acid (IC<sub>50</sub> = 49.08 μM), a representative tyrosinase inhibitor. A novel synthesized compound, (*E*)-2-((2,4-dihydroxyphenyl)diazenyl)phenyl 4-methylbenzenesulfonate (3), showed the best results with an IC<sub>50</sub> of 17.85 μM, and showed competitive inhibition on Lineweaver-Burk plots, as further confirmed by the docking results. In addition, active compounds 3–5 were not cytotoxic to cultured B16F10 cells at the concentrations tested, and inhibited both tyrosinase and melanin synthesis. Therefore the active compounds (3–5) might be considered excellent candidates for use in the development of therapeutic agents for diseases associated with hyperpigmentation.

**Key words:** tyrosinase inhibitor; resveratrol; azo-resveratrol; docking analysis; (*E*)-2-((2,4-dihydroxyphenyl)diazenyl)phenyl 4-methylbenzenesulfonate

The enzyme tyrosinase (EC1.14.18.1), a multifunctional, glycosylated, copper-containing metalloenzyme, is the key enzyme involved in the biosynthesis of the large biological pigment melanin.<sup>1)</sup> Melanin is formed by a combination of enzymatically catalyzed and chemical reactions. Tyrosinase exhibits monophenolase activity and diphenolase activity. That is, it catalyzes two divergent reactions of melanin biosynthesis, the hydroxylation of a monophenol and the conversion of an *O*-diphenol to the corresponding *O*-quinone. Thereby, it converts tyrosine to 3,4-dihydroxy-phenylalanine

(L-dopa), and oxidizes L-dopa to form dopaquinone. The former reaction is the rate-limiting step in melanin biosynthesis.<sup>2,3)</sup> This *O*-quinone, a highly reactive compound, can undergo spontaneous polymerization to form melanin.<sup>4)</sup>

Numerous naturally occurring and synthetic tyrosinase inhibitors, including arbutin,<sup>5)</sup> ascorbic acid derivatives,<sup>6)</sup> azeleic acid,<sup>7)</sup> hydroquinone,<sup>8)</sup> kojic acid,<sup>9)</sup> polyphenolic compounds,<sup>10–12)</sup> retinoids,<sup>13)</sup> and tetrahydroxystilbenes,<sup>14)</sup> have been reported, but most of these inhibitors either do not have sufficient potential activity to be of practical use, or are do not meet safety regulations for use as medicines and cosmetics. The clinical effectiveness of well-known active tyrosinase inhibitors, such as kojic acid and arbutin, has not yet been demonstrated.<sup>15,16)</sup> Due to its cytotoxic and mitogenic properties, hydroquinone, a widely used skin-lightening agent, is still controversial with regard to biosafety.<sup>17)</sup> Hence it remains necessary to search for and develop novel candidates demonstrating safe and potent activities that are devoid of side effects.

Resveratrol, 3,5,4'-trihydroxy-*trans*-stilbene, presents naturally at high concentrations in grape seeds and exhibits a wide range of biological and pharmacological activities, including antifungal, anticarcinogenesis, anti-aging, cardioprotective, and antioxidant effects.<sup>18–21)</sup> Some hydroxystilbene compounds, including oxyresveratrol and resveratrol, can also inhibit tyrosinase activity.<sup>22,23)</sup>

Hence we have conducted a search for easily accessible biological substances, including polyphenolic compounds, that can induce potent inhibition of tyrosinase activity and potentially prevent abnormal pigmentation.<sup>12,24)</sup> In addition, the interesting biological activities of resveratrol have prompted us to synthesize azo-resveratrol, and to evaluate its biological activities and compare them with those of resveratrol (Fig. 1).

<sup>†</sup> To whom correspondence should be addressed. Hae Young CHUNG, Tel: +82-51-510-2814; Fax: +82-51-518-2821; E-mail: hjung@pusan.ac.kr

\* These authors contributed equally to this work.

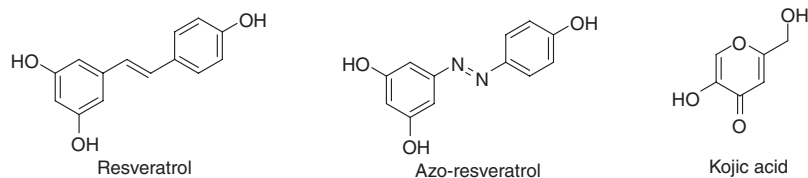


**Fig. 1.** Chemical Structures of Resveratrol, Azo-Resveratrol, and Kojic Acid.

The aim of the current study was to synthesize phenolic azo compounds as novel tyrosinase inhibitors, (*E*)-2-((substituted phenyl)diazenyl)phenyl 4-methylbenzenesulfonate derivatives (**2** and **3**) and (*E*)-2-((substituted phenyl)diazenyl)phenol derivatives (**4** and **5**), in order to study their potency as tyrosinase inhibitors and the kinetic mechanical parameters of inhibition, and to study their effects on melanin production and tyrosinase activity in the B16 murine melanoma cell line. In addition, using our compounds, we simulated the docking of mushroom tyrosinase. These results indicate that the affinity of the compounds for binding with tyrosinase is higher than that of kojic acid, used as control. Docking simulation suggested that the mechanism of compounds by Glu258, His261, and Asp276 showed possible hydrogen bonding interactions. The results should provide a basis for development of new effective skin-whitening agents with fewer adverse side effects.

## Materials and Methods

### Experimental.

**General.** Melting points are uncorrected.  $^1\text{H}$  and  $^{13}\text{C}$  NMR spectra were recorded on Varian Unity INOVA 400 and Varian Unity AS 500 instruments (Varian, Midland, ON). Chemical shifts are reported with reference to the respective residual solvent or deuterated peaks ( $\delta_{\text{H}}$  3.30 and  $\delta_{\text{C}}$  49.0 for  $\text{CD}_3\text{OD}$ ,  $\delta_{\text{H}}$  7.27 and  $\delta_{\text{C}}$  77.0 for  $\text{CDCl}_3$ ). Coupling constants are reported in hertz. The abbreviations used are as follows: s (singlet), br s (broad singlet), d (doublet), t (triplet), and dd (doublet of doublets). All of the reactions described below were performed under an argon or a nitrogen atmosphere, and were monitored by TLC. All anhydrous solvents were distilled over  $\text{CaH}_2$  or Na/benzophenone prior to use.

**2-Aminophenyl 4-methylbenzenesulfonate (1).**<sup>25</sup> Triethylamine (3.8 mL and 27.26 mmol) and *p*-toluenesulfonyl chloride (5.24 g, 27.48 mmol) were added subsequently to a stirred solution of 2-aminophenol (2.00 g, 18.33 mmol) in anhydrous THF (30 mL) at  $0^\circ\text{C}$ , and the reaction mixture was stirred at the same temperature overnight. Following partitioning of the reaction mixture between ethyl acetate and water, the organic layer was dried over anhydrous  $\text{MgSO}_4$ , filtered, and evaporated. The resulting residue was purified by silica gel column chromatography using hexane and ethyl acetate (6:1) as eluent to give *O*-tosyl product (4.80 g, 99%), an orange solid.

Melting point  $100.0$ – $101.5^\circ\text{C}$ ;  $^1\text{H}$  NMR (500 MHz,  $\text{CDCl}_3$ )  $\delta$  7.77 (d, 2 H,  $J = 8.5$  Hz, 2-H, 6-H), 7.32 (d, 2 H,  $J = 8.0$  Hz, 3-H, 5-H), 7.01 (t, 1 H,  $J = 7.5$  Hz, 4'-H), 6.79 (d, 1 H,  $J = 8.0$  Hz, 6'-H), 6.71 (d, 1 H,  $J = 7.5$  Hz, 3'-H), 6.59 (td, 1 H,  $J = 1.5, 7.5$  Hz, 5'-H), 3.83 (s, 2 H,  $\text{NH}_2$ ), 2.45 (s, 3 H, 4- $\text{CH}_3$ );  $^{13}\text{C}$  NMR (100 MHz,  $\text{CDCl}_3$ )  $\delta$  145.8 (C1'), 140.0 (C4), 137.1 (C2'), 132.8 (C1), 130.1 (C3, C5), 128.7 (C2, C6), 128.0 (C5'), 123.1 (C6'), 118.5 (C4'), 117.4 (C3'), 22.0 (4- $\text{CH}_3$ ).

**(E)-2-((4-Hydroxyphenyl)diazenyl)phenyl 4-methylbenzenesulfonate (2).** Tosylate **1** (150 mg, 0.57 mmol) was dissolved in a mixed solvent of THF (2 mL) and 1 M hydrochloric acid (1.5 mL). The solution was cooled to a temperature of  $0$ – $5^\circ\text{C}$  and diazotized by dropwise addition of sodium nitrite (47.2 mg, 0.68 mmol). After stirring for 30 min, the diazonium salt solution that formed was added in dropwise fashion to a pre-cooled ( $0$ – $5^\circ\text{C}$ ) solution of phenol (64.3 mg, 0.68 mmol) in 1 M NaOH (1.5 mL, 1.5 mmol). The reaction mixture was stirred for 3 h at  $0$ – $5^\circ\text{C}$ , followed by extraction with ethyl acetate.

The organic layer was dried over anhydrous  $\text{MgSO}_4$ , filtered, and evaporated under reduced pressure. The resulting residue, which was purified by silica gel column chromatography using hexane and ethyl acetate (3.5:1) as the eluent, gave tosylated diazo compound **2** (135 mg, 64%), a yellow oil.

UV (MeOH)  $\lambda_{\text{max}}$  282 nm;  $^1\text{H}$  NMR (500 MHz,  $\text{CDCl}_3$ )  $\delta$  7.64 (d, 2 H,  $J = 8.5$  Hz, 2''-H, 6''-H), 7.60 (d, 2 H,  $J = 8.5$  Hz, 2-H, 6-H), 7.56 (d, 1 H,  $J = 8.5$  Hz, 3'-H), 7.45–7.47 (m, 2 H, 4'-H, 6'-H), 7.36–7.32 (m, 1 H, 4'-H), 7.02 (d, 2 H,  $J = 8.5$  Hz, 3-H, 5-H), 6.91 (d, 2 H,  $J = 8.0$  Hz, 3''-H, 5''-H), 5.44 (s, 1 H, 4'-OH), 2.22 (s, 3 H,  $\text{CH}_3$ );  $^{13}\text{C}$  NMR (100 MHz,  $\text{CDCl}_3$ )  $\delta$  159.2 (C4''), 147.2, 146.9, 145.5, 145.3, 132.3 (C1), 131.4 (C5'), 129.8 (C3, C5), 128.6 (C2, C6), 128.0 (C3'), 125.8 (C2'', C6''), 124.9 (C4'), 117.5 (C6'), 115.6 (C3'', C5''), 21.8 (4- $\text{CH}_3$ ); HRMS (ESI)  $m/z$   $\text{C}_{19}\text{H}_{15}\text{N}_2\text{O}_4\text{S}$  (M – H)<sup>–</sup> calcd 367.0753, obsd 367.0746.

**(E)-2-((2,4-Dihydroxyphenyl)diazenyl)phenyl 4-methylbenzenesulfonate (3).** Compound **1** (150 mg, 0.57 mmol) was converted to compound **3** (74 mg, 34%), a yellow oil, by a procedure similar to that used in the preparation of compound **2**.

UV (MeOH)  $\lambda_{\text{max}}$  288 nm;  $^1\text{H}$  NMR (500 MHz,  $\text{CD}_3\text{OD}$ )  $\delta$  7.63 (dd, 1 H,  $J = 1.6, 8.0$  Hz, 3'-H), 7.55 (d, 2 H,  $J = 8.0$  Hz, 2-H, 6-H), 7.55 (d, 1 H,  $J = 9.0$  Hz, 6'-H), 7.47 (td, 1 H,  $J = 1.5, 8.0$  Hz, 5'-H), 7.42–7.39 (m, 2 H, 4'-H, 6'-H), 7.13 (d, 2 H,  $J = 8.0$  Hz, 3-H, 5-H), 6.52 (dd, 1 H,  $J = 2.5, 9.0$  Hz, 5''-H), 6.33 (d, 1 H,  $J = 2.5$  Hz, 3''-H), 2.23 (s, 3 H, 4- $\text{CH}_3$ );  $^{13}\text{C}$  NMR (100 MHz,  $\text{CD}_3\text{OD}$ )  $\delta$  164.2 (C4''), 156.8 (C2''), 146.2 (C1'), 144.9 (C4), 143.2, 134.8 (C5'), 133.3, 131.5, 130.3 (C6''), 129.6 (C3, C5), 128.4 (C2, C6), 128.0 (C3'), 124.4 (C4'), 117.2 (C6'), 109.5 (C5''), 102.8 (C3''), 20.4 (4- $\text{CH}_3$ ); HRMS (ESI)  $m/z$   $\text{C}_{19}\text{H}_{15}\text{N}_2\text{O}_5\text{S}$  (M – H)<sup>–</sup> calcd 383.0702, obsd 383.0707.

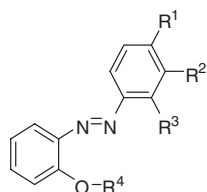
**(E)-2-((4-Hydroxyphenyl)diazenyl)phenol (4).**<sup>26,27</sup> Tosylated diazo compound **2** (52 mg, 0.14 mmol) was dissolved in 5% KOH w/w solution (1 mL), and the reaction mixture was refluxed for 1 h. Following the addition of 5% aqueous HCl solution for adjustment of the pH to 5–7, the reaction mixture was partitioned between ethyl acetate and water. The organic layer was dried over anhydrous  $\text{MgSO}_4$ , filtered, and concentrated under reduced pressure. To purify the resulting residue, silica gel column chromatography was performed using hexane and ethyl acetate (6.5:1), which afforded diazo compound **5** (28 mg, 92%), a red solid.

Melting point =  $113$ – $115^\circ\text{C}$ ; UV (MeOH)  $\lambda_{\text{max}}$  270 nm;  $^1\text{H}$  NMR (400 MHz,  $\text{CD}_3\text{OD}$ )  $\delta$  7.81 (dd, 1 H,  $J = 1.6, 8.0$  Hz, 3-H), 7.78 (d, 2 H,  $J = 8.8$  Hz, 2'-H, 6'-H), 7.29 (td, 1 H,  $J = 2.0, 8.0$  Hz, 5-H), 7.01 (td, 1 H,  $J = 1.6, 8.0$  Hz, 4-H), 6.94 (dd, 1 H,  $J = 1.2, 8.4$  Hz, 3-H), 6.91 (d, 2 H,  $J = 8.8$  Hz, 3'-H, 5'-H);  $^{13}\text{C}$  NMR (100 MHz,  $\text{CD}_3\text{OD}$ )  $\delta$  161.2 (C4'), 154.5 (C1), 144.4 (C1'), 137.5 (C2), 132.1 (C5), 130.7 (C3), 124.1 (C2', C6'), 119.7 (C4), 117.6 (C6), 115.9 (C3', C5').

**(E)-4-((2-Hydroxyphenyl)diazenyl)benzene-1,3-diol (5).**<sup>26,28</sup> Tosylated diazo compound **3** (43.8 mg, 0.11 mmol) was converted to compound **5** (8.0 mg, 30%), an orange solid, by a procedure similar to that used in the preparation of compound **4**.

Melting point =  $130.4$ – $133.1^\circ\text{C}$ ; UV (MeOH)  $\lambda_{\text{max}}$  282 nm;  $^1\text{H}$  NMR (500 MHz,  $\text{CD}_3\text{OD}$ )  $\delta$  7.72 (dd, 1 H,  $J = 1.5, 8.0$  Hz, 6'-H), 7.62 (d, 1 H,  $J = 9.0$  Hz, 5-H), 7.28 (td, 1 H,  $J = 1.5, 8.5$  Hz, 4'-H), 7.01–6.96 (m, 2 H, 3'-H, 5'-H), 6.50 (dd, 1 H,  $J = 2.5, 9.0$  Hz, 6-H), 6.34 (d, 1 H,  $J = 2.5$  Hz, 2-H);  $^{13}\text{C}$  NMR (100 MHz,  $\text{CD}_3\text{OD}$ )  $\delta$  163.2 (C1), 157.6 (C3), 152.6 (C2'), 136.1 (C1'), 131.5 (C4), 131.2 (C4'), 131.0 (C6'), 125.2 (C5), 119.9 (C5'), 117.5 (C3'), 109.1 (C6), 103.2 (C2) (Table 1).

**Materials.** Tyrosinase (EC1.14.18.1) from mushroom, L-tyrosine (L-Tyr), resveratrol (3,5,4'-trihydroxy-*trans*-stilbene), kojic acid [5-hydroxy-2-(hydroxymethyl)-4H-pyran-4-one], and  $\alpha$ -MSH (alpha-Melanocyte Stimulating Hormone) were purchased from Sigma (St. Louis, MO). All other chemicals and solvents were of analytical grade.

**Table 1.** Substitution Pattern and Inhibitory Effects on Mushroom Tyrosinase of the (*E*)-2-((Substituted phenyl)diazenyl)phenyl 4-Methylbenzenesulfonate and (*E*)-2-((Substituted phenyl)diazenyl)phenol Derivatives


Compound	R <sup>1</sup>	R <sup>2</sup>	R <sup>3</sup>	R <sup>4</sup>	Tyrosinase inhibition <sup>b</sup> (%)
<b>2</b>	OH	H	H	<sup>a</sup> Ts	34.03 ± 8.52
<b>3</b>	OH	H	OH	Ts	88.84 ± 3.03
<b>4</b>	OH	H	H	H	82.50 ± 1.68
<b>5</b>	OH	H	OH	H	75.22 ± 1.08
Kojic acid					56.16 ± 0.85

Values indicate means ± SE for three determinations.

<sup>a</sup>*p*-Toluenesulfonyl

<sup>b</sup>Tyrosinase inhibition was measured using L-tyrosine as substrate at 50 μM.

### Methods.

**Cell cultures.** B16F10 mouse melanoma cells, obtained from the Korean Cell Line Bank, were cultured in Dulbecco's Modified Eagle's Medium (DMEM; Gibco, Carlsbad, CA) containing 10% fetal bovine serum (FBS; Gibco) and penicillin/streptomycin (100 IU/50 μg/mL) in an incubator under a humidified atmosphere containing 5% CO<sub>2</sub>/95% air controlled at 37 °C. The cells were cultured in 24-well plates for use in assays for cell viability, melanin quantification, and enzyme activity.

**Cell viability assay.** To determine cell viability, a colorimetric cell proliferation assay was performed using 3-(4,5-dimethylthiazol-2-yl)-2,5-diphenyltetrazolium bromide (MTT) for measurement of mitochondrial activity in the viable cells. This method is based on the conversion of MTT (Sigma) to MTT-formazan crystals by a mitochondrial enzyme by a previously described method.<sup>29</sup> Briefly, cells were seeded at a density of 3 × 10<sup>4</sup> cells in a Corning 48-well plate and allowed to adhere overnight. The culture medium was then replaced with fresh serum-free DMEM. MTT was freshly prepared at 5 mg/mL in phosphate-buffered saline (PBS). Aliquots of 500 μL of MTT stock solution were added to each well, followed by incubation of the plate in an incubator at 37 °C under a humidified atmosphere containing 5% CO<sub>2</sub> for 4 h. Then, following removal of the medium, 500 μL of EtOH-DMSO (solution of a 1:1 mixture) was added to each well in order to dissolve the formazan. After 10 min, spectrophotometric measurement of the optical density of each well was performed using a 560 nm filter. The results for three determinations are shown Fig. 4.

**Assay of tyrosinase inhibitory activity.** Mushroom tyrosinase was used as the enzyme source for the entire study. Tyrosinase activity was determined by a previously described method, with minor modifications.<sup>30</sup> Briefly, 20 μL of an aqueous solution of mushroom tyrosinase (1,000 units) was added to a 96-well microplate (Nunc, Roskilde, Denmark), in a 200 μL assay mixture containing 1 mM L-tyrosine and 50 mM phosphate buffer (pH 6.5). The assay mixture was incubated at 25 °C for a period of 30 min. Following incubation, spectrophotometric measurement was done at 492 nm (OD<sub>492</sub>) using a microplate reader (Hewlett Packard, Palo Alto, CA) in order to determine the amount of dopachrome produced in the reaction mixture. IC<sub>50</sub> refers to the concentration of a substance that inhibits a standard response by 50% of the activity. The IC<sub>50</sub> value is derived experimentally from the X-axis on an inhibitor concentration *versus* the product formation curve, and is determined from the alignment of the dose-response curve on the dependent Y-axis. In the present study, dose-dependent inhibition experiments were performed in triplicate in order to determine the IC<sub>50</sub> values of the test compounds. Determination of log-linear curves and their equations was based on the average percentage inhibition for three doses. Average results for three determinations are shown.

**Kinetic analysis of the inhibition of tyrosinase.** Varying concentrations (0.25 to 2 mM) of L-tyrosine, a tyrosinase substrate, 20 μL of an

aqueous mushroom tyrosinase solution (1,000 units), and 50 mM potassium phosphate buffer (pH 6.5) with and without test samples (20 and 100 μM) were added to a 96-well plate in a total volume of 200 μL. With a microplate reader, the initial rate of dopachrome formation from the reaction mixture was determined by the increase in absorbance at a wavelength of 492 nm per min (ΔOD<sub>492</sub>/min). The Michaelis constant (*K<sub>m</sub>*), the maximal velocity (*V<sub>max</sub>*), and the inhibitor constant (*K<sub>i</sub>*) of tyrosinase activity were determined using a Lineweaver-Burk plot at varying concentrations of L-tyrosine.<sup>31</sup> Due to competitive inhibition by the compounds together with substrate inhibition by L-tyrosine, reaction kinetics required modification of the Michaelis-Menten equation. All experiments were performed in triplicate.

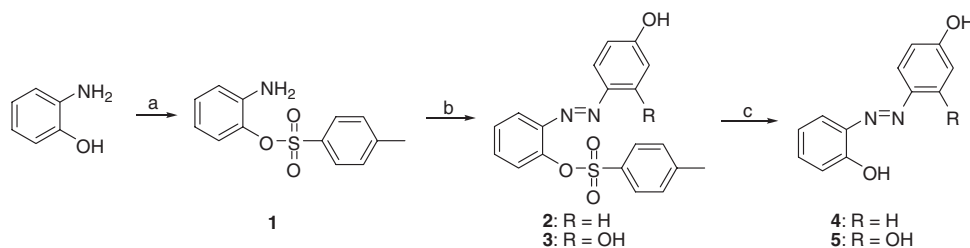
**Murine tyrosinase activity assay.** Measurement of the rate of L-DOPA oxidation was done to estimate tyrosinase activity.<sup>30</sup> Cells were plated in 24-well dishes at a density of 5 × 10<sup>4</sup> cells/mL. B16 cells were incubated in the presence and the absence of 100 nM α-MSH, followed by treatment for 24 h with various concentrations of compounds **3–5** (0–10 μM). Cells were washed and lysed in 100 μL of 50 mM sodium phosphate buffer (pH 6.5) containing 1% Triton X-100 (Sigma) and 0.1 mM PMSF (phenylmethylsulfonyl fluoride), and then frozen at –80 °C for 30 min. After thawing and mixing, cellular extracts were centrifuged for clarification at 12,000 rpm for 30 min at 4 °C.

An 8 μL sample of the supernatant and 20 μL of L-DOPA (2 mg/mL) were placed in a 96-well plate, and the absorbance was read at 492 nm every 10 min for 1 h at 37 °C using an enzyme-linked immunosorbent serologic assay (ELISA) plate reader. Final activity was expressed as ΔOD/min for each condition. The results of three determinations are shown.

**Melanin content assay.** Melanin content was used as an index of melanogenesis. The method described by Bilodeau *et al.*, with modifications, was used to determine melanin content.<sup>32</sup> In the present study, the amount of melanin was used as an index of melanogenesis. B16 cells (5 × 10<sup>4</sup>) were transferred to 24-well dishes and incubated in the presence and absence of 100 nM α-MSH. The cells were then incubated for 24 h with various concentrations of compounds **3, 4, and 5** (0–10 μM). After washing twice with PBS, samples were dissolved in 100 μL of 1 N NaOH. They were then incubated at 60 °C for 1 h and mixed in order to solubilize the melanin. The absorbance at 405 nm was compared with a standard curve for synthetic melanin. The results of three determinations are shown.

**Homology modeling of tyrosinase.** A three-dimensional model of *Lentinula edodes* (mushroom) tyrosinase, comprising 618 amino acids, was built using SWISS-MODEL based on homology modeling.<sup>33</sup> The SWISS-MODEL program automatically provides an all-atom model using alignments between the query sequence and known homologous structures. According to the known homologous structure of tyrosinase from the Protein Data Bank (PDB), 1BT3 (2.5 Å resolution) was used as structural template (15% sequence identity and e-value of 0.00e-1). By homology search between the target sequence and the total protein sequences in the PDB, the automated model of SWISS-MODEL automatically selected the 1BT3 structure as the best template. In order to validate the quality of the predicted structure model, we evaluated the Z-value using the QMEAN server (<http://swissmodel.expasy.org/qmean>). To prepare a docking simulation, we performed deletion of solvent, addition of hydrogen, addition of charge, and replacement of the incomplete side chain of the structure model using the Chimera program (<http://www.cgl.ucsf.edu/chimera/>). For addition of charge, we used the charge data of AMBER ff99SB for standard residues.

**In silico docking of tyrosinase and target compounds.** For docking simulation, we used the AutoDock4.2 program. Among the many tools available for *in silico* protein-ligand docking, AutoDock4.2 is the most commonly used due to its automated docking capability.<sup>34</sup> To define the docking pocket, we used a set of predefined active sites which got from the tyrosinase structure of *Bacillus megaterium* in complex with kojic acid as the inhibitor. We attempted to perform a docking simulation of tyrosinase and the compounds, with kojic acid as the reference inhibitor. To prepare of compounds for the docking simulation, we performed the following steps: (1) conversion of 2D structures into 3D structures, (2) calculation of charges, and (3) the addition of hydrogen atoms using the ChemOffice program (<http://www.cambridgesoft.com>).



**Scheme 1.** Synthesis of Target Compounds.

Reagents and conditions: (a) *p*-TsCl, Et<sub>3</sub>N, THF, room temperature, overnight, 99%; (b) NaNO<sub>2</sub>, 1 M HCl, THF, 0–5 °C, 30 min, and then phenol, 1 M NaOH, 0–5 °C, 3 h, 64% for **2**, 1,3-dihydroxybenzene, 1 M NaOH, 0–5 °C, 3 h, 34% for **3**; (c) 5% KOH, reflux, 1 h, 92% for **4**, 4 h, 30% for **5**.

*Shared pharmacophore of the target compounds.* Pharmacophore is an ensemble of ligand features that is necessary for interaction with a specific receptor in any biological response.<sup>35)</sup> Because three of the compounds had similar chemical structures and kinetic responses for tyrosinase inhibition, we searched the pharmacophore of the target compounds. A pharmacophore model was generated using the LigandScout 3.0 program.<sup>36)</sup> On the basis of the type of atom, the chemical features of the target compounds were defined according to various pharmacophore elements, including hydrogen bond acceptor, hydrogen bond donor, positive ionizable area, negative ionizable area, hydrophobic interactions, and aromatic ring. Specifically, we searched shared pharmacophores by alignment of the predicted pharmacophores of the target compounds.

*Statistical analysis.* Inhibition of tyrosinase activity was expressed as a percentage of inhibition based on  $100 - [(A \times 100)/B]$ , where  $A = OD_{492}$  with a test sample and  $B = OD_{492}$  without a test sample. The data collected had a mean standard error ( $n = 3$ ). One-factor analysis of variance (ANOVA) followed by the Fisher's protected least significant difference *post hoc* test was used to determine statistical significance of differences among groups. Values of  $*p < 0.05$  were considered statistically significant.

## Results

### Synthesis of azo compounds (1–5)

A strategy for the synthesis of diaryl azo compounds is outlined in Scheme 1. It was envisioned that azo compounds can be synthesized from the aryl diazonium ion, obtained from the reaction of an aniline derivative with sodium nitrite under acidic conditions and phenolic analogs. 2'-Hydroxyaniline was selected as the starting material for the preparation of diazonium salt. In order to prevent side reactions, an appropriate group must be used to protect the hydroxyl group. Because the diazotization reaction proceeds under acidic conditions, acetyl and silyl, which are unstable in acidic conditions, cannot be used as a protecting group for the hydroxyl group on a phenolic compound. Of ether and sulfonate functionalities, which are stable under acidic conditions, sulfonate was chosen, because in case of protection with ether functionality, extremely strong acidic conditions were required in order to deprotect the bond after formation of the diaryl azo compound. According to the literature,<sup>37)</sup> by the proper choice of a base, selective *O*-tosylation in the presence of a free amine or *N*-tosylate in the presence of a free hydroxyl is possible at good yields. Treatment of 2'-hydroxyaniline with *p*-TsCl in the presence of triethylamine in THF gave *O*-tosylate **2**, at a yield of 99%, a sulfonate-protected aniline, which in turn was diazotized with sodium nitrite under acidic conditions to afford diazonium salt. The reaction of diazonium salt with phenolic compounds, including phenol and 2,4-dihydroxybenzene, under weak basic

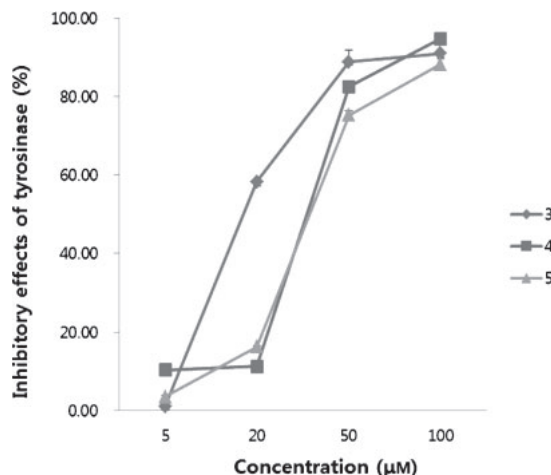


**Fig. 2.** Dose-Dependent Inhibitory Effects of Compounds **3**, **4**, and **5** against Mushroom Tyrosinase.

L-Tyrosine was used as substrate for the measurement of tyrosinase activity. Compounds **3** (diamonds), **4** (rectangles), and **5** (triangles) were found to be inhibitors of tyrosinase. The effects of various concentrations of compounds (5–100 µM) on tyrosinase activity are represented as % inhibition and mean  $\pm$  SE of three determinations.

conditions resulted in the generation of 4-hydroxyphenyl and 2,4-dihydroxyphenyl azo compounds **2** and **3** respectively, yields of 64% and 34%, indicating that the *para*-position of the hydroxyl group on an aromatic ring is more nucleophilic than its *ortho*- or *meta*-position. Removal of the tosyl group was accomplished by refluxing compounds **2** and **3** in 5% KOH aqueous solution, affording 4-hydroxyphenyl and 2,4-dihydroxyphenyl azo compounds **4** and **5** respectively.

### Inhibitory effects of compounds **2**, **3**, **4**, and **5** on mushroom tyrosinase

These (*E*)-2-((substituted phenyl)diazanyl)phenyl 4-methylbenzenesulfonate and (*E*)-2-((substituted phenyl)diazanyl)phenol derivatives showed strong tyrosinase inhibition as compared to that of kojic acid, used as positive control when the enzymatic reactions used L-tyrosine as substrate. The results of the inhibition of tyrosinase using these compounds are shown in Table 1. Our results indicate that three out of the four compounds (compounds **2**, **3**, **4**, and **5**) showed significant inhibition activity of mushroom tyrosinase greater than that of kojic acid. As shown in Fig. 2, active compounds **3**, **4**, and **5** induced dose-dependent reductions in tyrosinase activity (5–100 µM). In particular, novel compound **3** showed the most potent inhibitory activity, with an IC<sub>50</sub>

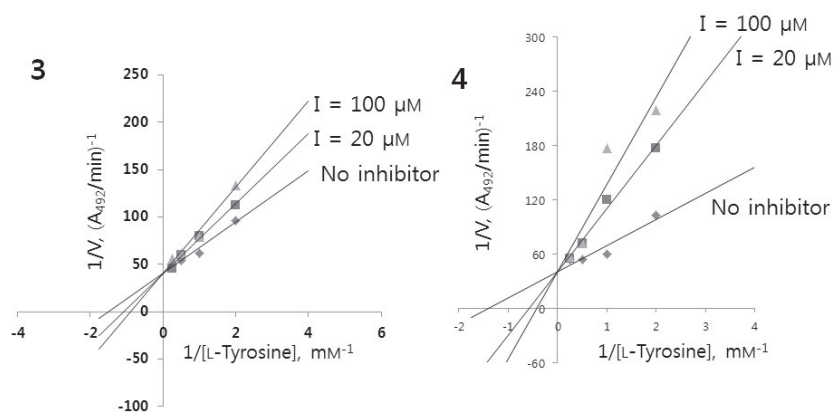


**Fig. 3.** Effects on Mushroom Tyrosinase Activity and Determination of the Inhibitory Mechanism.

The equation for the Lineweaver–Burk plot is  $1/V = K_m/V_{max} \times 1/[S] + 1/V_{max}$ , and the modified Michaelis–Menten equation is  $1/V_{max} = 1/K_m(1 + [I]/K_i)$ , where  $V$  is the reaction velocity,  $K_m$  is the Michaelis–Menten constant,  $V_{max}$  is the maximum reaction velocity,  $[S]$  is the substrate concentration,  $[I]$  is the inhibitor concentration, and  $K_i$  is the inhibition constant.

**Table 2.** Kinetic Analysis of Active Compounds

Compound	IC <sub>50</sub> <sup>a</sup> (μM)	Type of inhibition <sup>b</sup>	K <sub>m</sub> <sup>c</sup> (mM)	K <sub>i</sub> <sup>c</sup> (μM)
<b>2</b>	200.77 ± 2.75	Competitive	1.19	27.60
<b>3</b>	17.85 ± 0.17	Competitive	0.93	54.40
<b>4</b>	44.11 ± 0.88	Competitive	1.74	14.17
<b>5</b>	48.29 ± 0.59	Competitive	1.26	26.67
Kojic acid	49.08 ± 0.36	—	—	—
Resveratrol	59.80 ± 0.98	—	—	—

Lineweaver-Burk plots for inhibition of the compounds on mushroom tyrosinase. Data were obtained as mean values of  $1/V$ , the inverse of the absorbance increase at a wavelength of 492 nm per min, for three independent tests using various concentrations of L-tyrosine substrate.

<sup>a</sup>50% inhibitory concentration (IC<sub>50</sub>).

<sup>b</sup>Lineweaver-Burk plot for mushroom tyrosinase.

<sup>c</sup>Values were measured at 20 μM of active compounds.

value of 17.85 μM, while those of kojic acid and resveratrol, used as positive controls, were 49.08 and 59.80 μM respectively (Table 2).

#### Active compounds inhibitory of mushroom tyrosinase with L-tyrosine as substrate

Because active compounds were investigated to identify very strong tyrosinase inhibition activity, analysis of kinetic behavior during the oxidation of L-tyrosine was done by Lineweaver-Burk plot assay (Fig. 3). Plots of the initial rates of tyrosinase activity in the presence of increasing concentrations of L-tyrosine yielded a family of straight lines of different slopes intersecting one point on the Y axis. Because the concentration of L-tyrosine substrate varied, the  $K_m$  value for tyrosinase showed a dose-dependent increase without any change in the  $V_{max}$  value, regardless of the concentration of compounds **2–5**, indicating that (Table 2). Many tyrosinase inhibitors have been found to be competitive inhibitors by chelating the copper in the active site of the enzyme.<sup>38,39</sup> Hence we assumed that compounds **2–5** can induce inhibition in a similar manner, but further study is necessary in order to support this assumption.

#### Effects of active compounds **3**, **4**, and **5** on the viability of B16F10 melanoma cells

We examined the cytotoxicity of compounds **3**, **4**, and **5**, which exhibited strong tyrosinase inhibition, in order

to determine whether the inhibitors would adversely induce B16F10 melanoma cell death. A cell viability assay using MTT was done to estimate cytotoxic effects, as shown in Fig. 4A. The results indicate that these compounds showed no significant cytotoxic effect in B16F10 melanoma cells at any of the concentrations tested, indicating that these compounds are relatively non-cytotoxic under the experimental conditions used for the examinations of melanin content and tyrosinase activity.

#### Effects of compounds **3**, **4**, and **5** on melanin production in B16F10 melanoma cells

The inhibitory potency of active compounds **3**, **4**, and **5** against melanin synthesis, we quantified the melanin contents of cultured B16F10 cells in the presence of 1, 5, and 10 μM compounds **3–5**. α-MSH, which stimulates melanogenesis, was used at 100 nM as negative control and its effect on melanin production was compared with that of the active compounds in the presence of 100 nM α-MSH. Melanin synthesis in the B16F10 melanoma cells treated with these compounds showed a significant reduction. The inhibitory influence of these compounds on melanin content is shown in Fig. 4B. The percentages of melanin content of compounds **3–5** in the cells were, respectively, 157.54%, 171.0%, 153.92% at 1 μM, 132.61%, 171.67%, 132.22% at 5 μM, and 131.73%, 113.28%, 121.58% at 10 μM, as compared to 100 nM α-MSH alone (269.87%) and the control (100%). Thus data from the cell viability test (Fig. 4A) indicate effective suppression of melanin production by active compounds **3**, **4**, and **5**, with less or no cytotoxicity.

#### Inhibitory effects of tyrosinase activity in B16F10 melanoma cells by active compounds

To determine the inhibitory mechanisms of the inhibition of melanin biosynthesis by compounds **3**, **4**, and **5**, the effect of compounds **3–5** on cellular tyrosinase activity in the B16F10 melanoma cells treated with α-MSH was examined. As shown in Fig. 4C, we found that compounds **3–5** had inhibitory effects on α-MSH-stimulated tyrosinase activity. After 24 h of incubation with compound **3**, tyrosinase activity was 154.97% at 1 μM, 125.80% at 5 μM, and 109.24% at

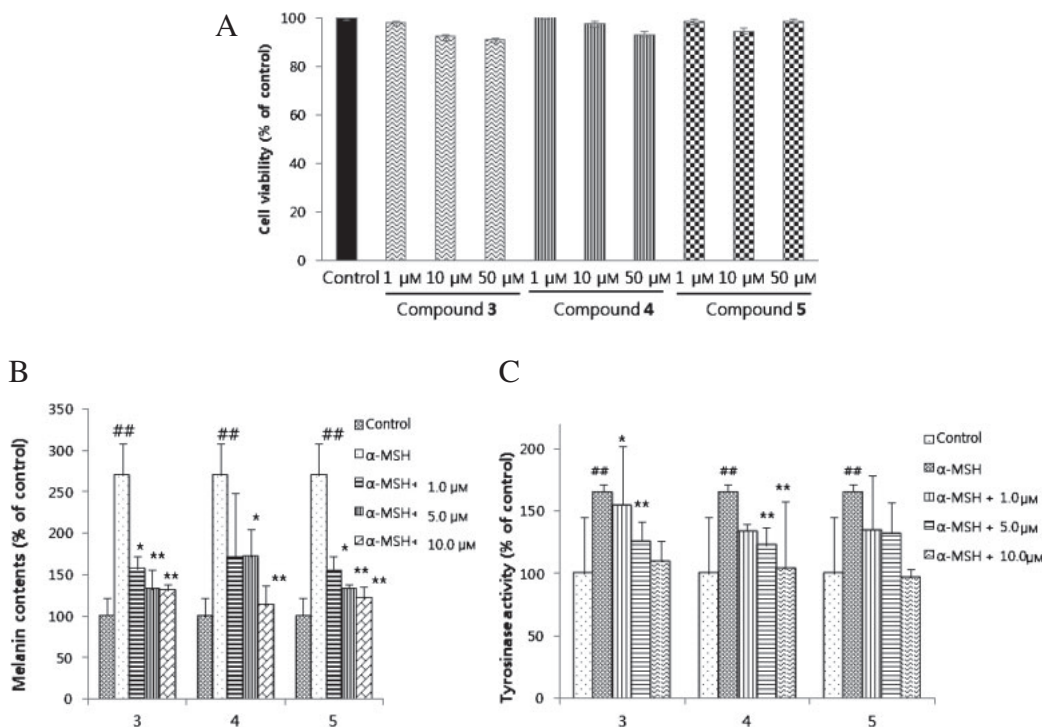


**Fig. 4.** Effects of Compounds **3**, **4**, and **5** on Cell Viability, Melanin Synthesis, and Tyrosinase Activity in B16F10 Melanoma Cells.

A, Cells were treated with various concentrations of compounds **3**, **4**, and **5** (0–50  $\mu\text{M}$ ), followed by examination by MTT assay. Each value represents the mean  $\pm$  SE for three determinations. Data are expressed as % cell viability. B, Measurement of the amount of melanin was done as described in “Materials and Methods.” C, B16 cells were harvested and tyrosinase activity was measured. Data are expressed as percentages of control, and values are expressed as mean  $\pm$  SE for three determinations. ##  $p < 0.01$  vs. the untreated control group; \*  $p < 0.05$ , and \*\*  $p < 0.01$  vs. the 100 nM  $\alpha$ -MSH treatment group.

10  $\mu\text{M}$ , while that of the control group treated with  $\alpha$ -MSH alone was 165.59%.

#### Molecular docking study of active compounds

To the predicted structure model, we evaluated the Z-score of the 3D structure using the QMEAN server. Because mushroom tyrosinase showed low sequence identity (15%) with the template structure (3NQ1), the Z-score for the predicted model was  $-4.8$ . However, we evaluated the quality of each residue on the tyrosinase structure (data not shown). The internal region, which was bound with kojic acid and compounds, was more reliable (blue) than the external region (red) of tyrosinase. The estimated residue error was visualized using a color gradient from blue (more reliable regions) to red (potentially unreliable regions, estimated error above 3.5  $\text{\AA}$ ). The docking simulation was successful, with significant scores. The binding energies of compounds were  $-5.94$  kcal/mol (**2**),  $-5.70$  kcal/mol (**3**),  $-5.10$  kcal/mol (**4**), and  $-4.57$  kcal/mol (**5**), and the binding energy of kojic acid was  $-2.73$  kcal/mol. The docking score between the ligand and the receptor is represented by various energy terms, such as electrostatic energy, van der Waals energy, and salvation energy. In particular, the docking simulation confirmed that the binding affinity of compounds **2–5** was higher than that of kojic acid, which was used as control. In addition, we determined the differences, in docking position of kojic acid and the compounds. The distances between the copper ions and the compounds, were 6.7  $\text{\AA}$  (kojic acid), 7.5  $\text{\AA}$  (**2**), 7.7  $\text{\AA}$  (**3**), 6.3  $\text{\AA}$  (**4**), and 8.0  $\text{\AA}$  (**5**) (Fig. 5A). In addition, we searched for hydrogen binding interaction between tyrosinase and the com-

pounds, and kojic acid. Only the Asp262 residue of tyrosinase was mainly responsible for the hydrogen bonding interactions with kojic acid. However, of the compounds, the Glu258 (**4**), His261 (**4**, **3**, **2**), and Asp276 (**3**, **2**) residues of tyrosinase were predicted as bonding interactions with the compounds (Fig. 5B). The residues functioned, as key residues and had an effect on binding affinity. Shared pharmacophore results confirmed the hydrogen bonding interaction of the docking simulation. The target compounds shared one donor and three acceptors of hydrogen bonding (Fig. 5C).

## Discussion

Melanin plays an important role in the protection of human skin from the harmful effects of UV radiation from the sun. Melanin is also a determinant of a person’s phenotypic appearance. Although it has mainly a photoprotective function in human skin, accumulation of an abnormal amount of melanin in different specific parts of the skin, resulting in a greater number of pigmented patches, can become an esthetic problem. Hyperpigmentation, such as melasma, ephelide, and lentigo in human skin and enzymatic browning in fruits and vegetables is not desirable. The occurrence of these phenomena has encouraged researchers to seek potent new safe tyrosinase inhibitors for use in anti-browning in farm products<sup>40</sup>) and skin whitening for medicinal<sup>41</sup>) and cosmetic purposes.<sup>42</sup>) Recent expansion of the global market has resulted in an ever-growing demand for new products for depigmentation, cosmeceutical, and skin lightening purposes.<sup>43</sup>)

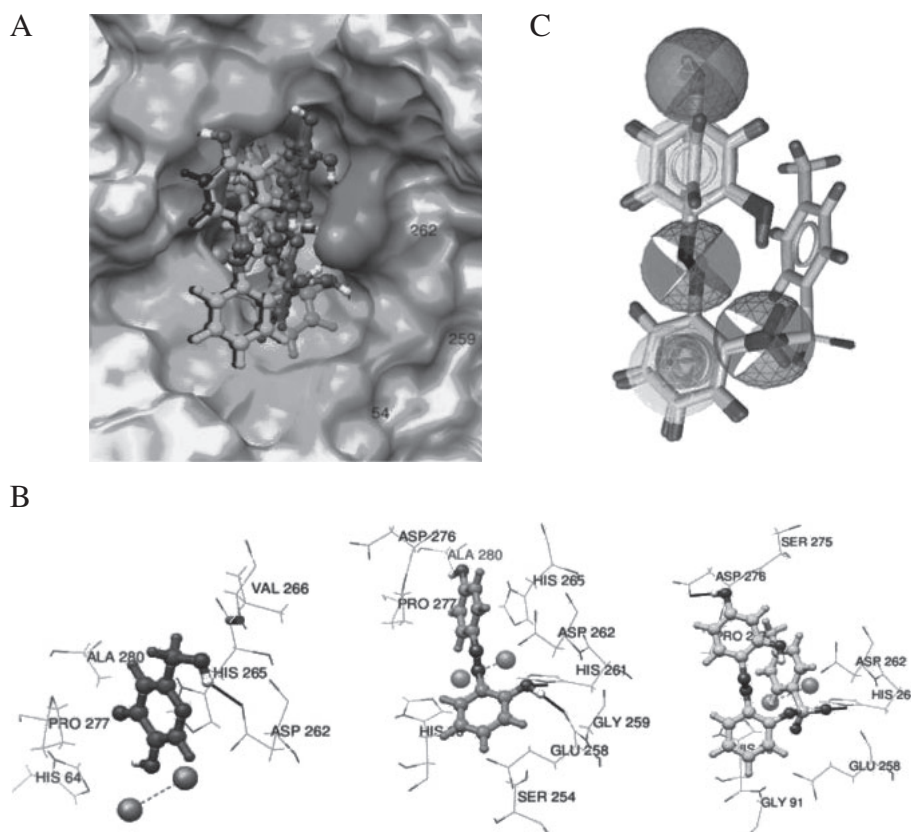


**Fig. 5.** Docking Simulation between Tyrosinase and Target Compounds.

A, Yellow zone is the active site. Gold ball is the copper ion. Magenta compound is kojic acid, which was used as control compound. Blue, yellow, cyan, and red compounds are **2**, **3**, **4**, and **5** respectively. B, Possible hydrogen binding interaction between tyrosinase and target compounds. C, The pharmacophore model was generated using the LigandScout 3.0 program. Red, green, and yellow phores represent a hydrogen bond acceptor, a hydrogen bond donor, and a hydrophobic region respectively.

In anticipation of finding an effective new substance for skin whitening and the prevention of hyperpigmentation, we synthesized (*E*)-2-((substituted phenyl)diazenyl)phenyl 4-methylbenzenesulfonate and (*E*)-2-((substituted phenyl)diazenyl)phenol derivatives (Table 1), and investigated the effects of our derivatives on tyrosinase inhibition. Three compounds, **3–5**, showed more potent dose-dependent inhibitory activity against mushroom tyrosinase than kojic acid and resveratrol, used as positive controls (Fig. 2 and Table 2). We also found that compound **3**, which was newly synthesized, gave the best results. A tosyl group as a protecting group is compatible with both a diazotization reaction and a sequential coupling reaction with phenolic compounds, and is easily removed under reflux in basic conditions. This finding might be helpful in the synthesis of azo-resveratrol which is our next target compound. The results of a kinetic study of inhibition of mushroom tyrosinase by our compounds indicated competitive inhibition of the enzyme, meaning that the compound binds to the active site of the enzyme (Fig. 3).<sup>44)</sup> Due to structural similarity to tyrosinase substrates, the inhibitory mode of phenolic compounds, the largest group of tyrosinase inhibitors to date, is usually competitive inhibition.<sup>45,46)</sup>

A homology modeling program was used to predict the tertiary structure of tyrosinase, and simulated docking of mushroom tyrosinase was done using our compounds (Fig. 5A). The results suggest that the affinity of the compounds for binding with tyrosinase

is higher than that of kojic acid which was used as control. A docking simulation suggested that the mechanism of compounds by Glu258, His261, and Asp276 had possible hydrogen bonding interactions (Fig. 5B). A shared pharmacophore model underlined the features of the four compounds, which had one donor and three acceptors of hydrogen bond (Fig. 5C). The docking results a pharmacophore model, and this clarified the key features required for optimal tyrosinase inhibition. No cytotoxicity of active compounds **3–5** was observed in cultured B16F10 melanoma cells up to 50  $\mu\text{M}$  (Fig. 4A). Dose-dependent suppression of tyrosinase activity and melanin synthesis was observed at concentrations ranging from 1 to 10  $\mu\text{M}$  (Fig. 4B and C), the proposed mechanism of tyrosinase inhibition of active compounds. Thus compounds **3–5** with an honest effort inhibited, melanin production at concentrations that did not significantly affect cell viability. In a previous study, we examined the inhibitory effects of kojic acid on tyrosinase activity and melanin contents in  $\alpha$ -MSH-treated B16F10 melanoma cells. We also found that kojic acid did not inhibit tyrosinase activity and did not affect the level of melanin contents in comparison with the level in the group treated with  $\alpha$ -MSH only.<sup>47)</sup> These cell-based experiments indicate that compounds **3–5** are much better whitening agents than kojic acid.

Based on the results of the present study, we conclude that a series of azo-resveratrol compounds were synthesized, and that compounds **2–5** were competitive inhibitors of mushroom tyrosinase. A docking simula-

tion with mushroom tyrosinase indicated that the binding affinities of compounds **2–5** were even higher than that of kojic acid, and a shared pharmacophore model indicated that the compounds had one donor and three acceptors for the hydrogen bond in common. These findings should give researchers help in developing potent tyrosinase inhibitors. Three azo-resveratrol analogs, **3–5**, with potent mushroom tyrosinase inhibitory activity also induced inhibition of cellular tyrosinase activity and melanin production in murine B16F10 melanoma cells. In particular, newly synthesized *(E)*-2-((2,4-dihydroxyphenyl) diazenyl)phenyl 4-methylbenzenesulfonate (**3**), showing an IC<sub>50</sub> of 17.85 ± 0.17 μM, was more effective than kojic acid and resveratrol, and hence might be considered an excellent candidate for use as a therapeutic agent for anti-melanogenesis. Further studies for the development of active compounds **3–5** as promising therapeutic materials for the control of abnormal skin pigmentation are warranted.

## Acknowledgments

This work was supported by a 2-Year Research Grant of Pusan National University.

## References

- Bao K, Dai Y, Zhu ZB, Tu FJ, Zhang WG, and Yao XS, *Bioorg. Med. Chem.*, **18**, 6708–6714 (2010).
- Fenoll LG, Rodríguez-López JN, García-Sevilla F, García-Ruiz PA, Varón R, García-Cánovas F, and Tudela J, *Biochim. Biophys. Acta*, **1548**, 1–22 (2001).
- Hearing VJ and Tsukamoto K, *FASEB J.*, **5**, 2902–2909 (1991).
- Solano F, Briganti S, Picardo M, and Ghanem G, *Pigment Cell Res.*, **19**, 550–571 (2006).
- Nakajima M, Shinoda I, Fukuwatari Y, and Hayasawa H, *Pigment Cell Res.*, **11**, 12–17 (1998).
- Kameyama K, Sakai C, Kondoh S, Yonemoto K, Nishiyama S, Tagawa M, Murata T, Ohnuma T, Quigley J, Dorsky A, Bucks D, and Blanock K, *J. Am. Acad. Dermatol.*, **34**, 29–33 (1996).
- Hermanns JF, Petit L, Pierard-Franchimont C, Paquet P, and Pierard GE, *Dermatology*, **204**, 281–286 (2002).
- Garcia A and Fulton JE Jr, *Dermatol. Surg.*, **22**, 443–447 (1996).
- Cabanes J, Chazarra S, and Garcia-Carmona F, *J. Pharm. Pharmacol.*, **46**, 982–985 (1994).
- Ohguchi K, Tanaka T, Iliya I, Ito T, Inuma M, Matsumoto K, Akao Y, and Nozawa Y, *Biosci. Biotechnol. Biochem.*, **67**, 663–665 (2003).
- Roh JS, Han JY, Kim JH, and Hwang JK, *Biol. Pharm. Bull.*, **27**, 1976–1978 (2004).
- No JK, Kim MS, Kim YJ, Bae SJ, Choi JS, and Chung HY, *Am. J. Chin. Med.*, **32**, 1–7 (2004).
- Yoshimura K, Tsukamoto K, Okazaki M, Virador VM, Lei TC, Suzuki Y, Uchida G, Kitano Y, and Harii K, *J. Dermatol. Sci.*, **27**, S68–S75 (2001).
- Ohguchi K, Tanaka T, Kido T, Baba K, Inuma M, Matsumoto K, Akao Y, and Nozawa Y, *Biochem. Biophys. Res. Commun.*, **307**, 861–863 (2003).
- Burnett CL, Bergfeld WF, Belsito DV, Hill RA, Klaassen CD, Liebler DC, Marks JG Jr, Shank RC, Slaga TJ, Snyder PW, and Andersen FA, *Int. J. Toxicol.*, **29**, S244–S273 (2010).
- Halder RM and Richards GM, *Skin Therapy Lett.*, **9**, 1–3 (2004).
- Draeos ZD, *Dermatol. Ther.*, **20**, 308–313 (2007).
- Murcia MA and Martínez-Tomé M, *J. Food Prot.*, **64**, 379–384 (2001).
- Bernard P and Berthon JY, *Int. J. Cosmet. Sci.*, **22**, 219–226 (2000).
- Athar M, Back JH, Tang X, Kim KH, Kopelovich L, Bickers DR, and Kim AL, *Toxicol. Appl. Pharmacol.*, **224**, 274–283 (2007).
- Hung LM, Su MJ, Chu WK, Chiao CW, Chan WF, and Chen JK, *Br. J. Pharmacol.*, **135**, 1627–1633 (2002).
- Ohguchi K, Tanaka T, Kido T, Baba K, Inuma M, Matsumoto K, Akao Y, and Nozawa Y, *Biochem. Biophys. Res. Commun.*, **307**, 861–863 (2003).
- Shin NH, Ryu SY, Lee HS, Min KR, and Kim YS, *Planta Med.*, **64**, 283–284 (1998).
- Kim YJ, No JK, Lee JH, and Chung HY, *Biol. Pharm. Bull.*, **28**, 323–327 (2005).
- Downer-Riley NK and Jackson YA, *Tetrahedron*, **63**, 10276–10281 (2007).
- Diehl H and Ellingboe J, *Anal. Chem.*, **32**, 1120–1123 (1960).
- Polyak B, Geresh S, and Marks RS, *Biomacromolecules*, **5**, 389–396 (2004).
- Berber H, Ogretir C, Lekesiz ECS, and Ermis E, *J. Chem. Eng. Data*, **53**, 1049–1055 (2008).
- Tada H, Shiho O, Kuroshima K, Koyama M, and Tsukamoto K, *J. Immunol. Methods*, **93**, 157–165 (1986).
- No JK, Soung DY, Kim YJ, Shim KH, Jun YS, Rhee SH, Yokozawa T, and Chung HY, *Life Sci.*, **65**, PL241–PL246 (1999).
- Kim DS, Kim SY, Chung JH, Kim KH, Eun C, and Park KC, *Cell Signal.*, **14**, 779–785 (2002).
- Bilodeau ML, Greulich JD, Hullinger RL, Bertolotto C, Ballotti R, and Andrisani OM, *Pigment Cell Res.*, **14**, 328–336 (2001).
- Rodríguez R, China G, Lopez N, Pons T, and Vriend G, *Bioinformatics*, **14**, 523–528 (1998).
- Morris GM, Goodsell DS, Halliday RS, Huey R, Hart WE, Belew RK, and Olson AJ, *J. Comput. Chem.*, **19**, 1639–1662 (1998).
- Wermuth CG, Ganellin CR, Lindberg P, and Mitscher LA, *Pure Appl. Chem.*, **70**, 1129–1143 (1998).
- Wolber G and Langer T, *J. Chem. Inf.*, **45**, 160–169 (2005).
- Kurita K, *Chem. Ind. (London)*, **8**, 345 (1974).
- Son SM, Moon KD, and Lee CY, *J. Agric. Food Chem.*, **48**, 2071–2074 (2000).
- Battaini G, Monzani E, Casella L, Santagostini L, and Pagliarini R, *J. Biol. Inorg. Chem.*, **5**, 262–268 (2000).
- Kubo I, Kinst-Hori I, Nihei K, Soria F, Takasaki M, Calderón JS, and Céspedes CL, *Z. Naturforsch. C*, **58**, 719–725 (2003).
- Gasowska-Bajger B and Wojtasek H, *Bioorg. Med. Chem. Lett.*, **18**, 3296–3300 (2008).
- Cho YH, Kim JH, Park SM, Lee BC, Pyo HB, and Park HD, *J. Cosmet. Sci.*, **57**, 11–21 (2006).
- Gandía-Herrero F, Jiménez M, Cabanes J, García-Carmona F, and Escribano J, *J. Agric. Food Chem.*, **51**, 7764–7769 (2003).
- Ha YM, Park YJ, Lee JY, Park D, Choi YJ, Lee EK, Kim JM, Kim JA, Park JY, Lee HJ, Moon HR, and Chung HY, *Biochimie*, **94**, 533–540 (2012).
- Kubo I and Kinst-Hori I, *J. Agric. Food Chem.*, **47**, 4121–4125 (1999).
- Kubo I, Kinst-Hori I, Chaudhuri SK, Kubo Y, Sánchez Y, and Ogura T, *Bioorg. Med. Chem.*, **8**, 1749–1755 (2000).
- Ha YM, Kim JA, Park YJ, Park D, Kim JM, Chung KW, Lee EK, Park JY, Lee JY, Lee HJ, Yoon JH, Moon HR, and Chung HY, *Biochim. Biophys. Acta*, **6**, 612–619 (2011).